Experimental and modeling investigation of the effect of ventilation on smoke rollback in a mine entry

J.C. EDWARDS, R.A. FRANKS, G.F. FRIEL AND L. YUAN

J.C. Edwards, member SME, **R.A. Franks**, **G.F. Friel** and **L. Yuan** are research physicist, electronics engineer, chemical engineer and associate service fellow, respectively, with the National Institute for Occupational Safety and Health, Pittsburgh Research Laboratory, Pittsburgh, PA. Preprint number 05-014, presented at the SME Annual Meeting, Feb. 25-March 2, 2005, Salt Lake City, UT. Revised manuscript received November 2005 and accepted for publication December 2005. Discussion of this peer-reviewed and approved paper is invited and must be submitted to SME Publications Dept. prior to July 31, 2006.

Introduction

An underground mine fire can have devastating consequences for miners and the mine if not controlled in its incipient stage. Inhalation of the fire-generated toxic products of combustion (POC) can be injurious or fatal for miners, and the heat released can induce roof and rib collapses. Initially, the thermal buoyancy forces generated by the fire will produce an ascending plume of fire POC. With sufficient ventilation, the POC will initially be transported downwind from the fire. Once the fire has evolved to sufficient intensity, the buoyancy forces will overcome the inertial forces of the ventilation, and the POC will migrate upwind along the roof counter to the positive ventilation. As noted by Mitchell (1996), smoke from mine fires always rolls back in sufficiently low airflows and can contain combustible gases that are subject to ignition by the mine fire when diluted by air. This poses a risk for the firefighters. The ventilation velocity, airway dimensions, airway slope and fire intensity determine the extent of smoke rollback along the roof into the fresh air.

Moderately small quantities of fuel can generate significant heat and smoke. A diesel fuel spill covering a 0.93-m- (3-ft-) diameter circular area would generate a 1-MW fire source. Similarly, a conical pile of broken coal with a 4.57-m- (15-ft-) diameter at the base and a height of 1.83 m (6-ft) would generate a 1.5 MW fire. A 2.4-m- (7.9-ft-) high wood crib consisting of 1.22-m- (4-ft-) long, 0.15-m- (0.5-ft-) square timbers can generate a 3.5-MW fire.

The smoke layer above the fire will simultaneously thicken as the rollback occurs. Not only can the smoke prevent direct access to the fire, it can leak through stoppings into adjacent airways and thereby further endanger the miners. One extreme consequence of a further increase in the fire intensity is that a sufficiently large heat production rate can produce flow reversal in an intake airway if the airway connects with parallel intake airways. The parallel airways could carry the balance of the airflow to substantially maintain the prefire mine pressure drop.

The use of ventilation to control the movement and dilution of smoke associated with an underground mine fire is recommended, but not quantified. Ventilation control, for example, is a recommended method (Code of Federal Regulations, 2002) for the control of toxic products from shop areas in metal and nonmetal mines. However, a quantified ventilation strategy is not generally available for implementation. The primary reaction is egression from the mine fire region. Even under the best of circumstances, miners are often required to egress through a toxic low-visibility mine atmosphere produced by the mine fire. Similarly, any attempt to approach the fire from the intake side for its control and suppression will be thwarted by low-visibility smoke conditions and toxic fire products, principally carbon monoxide (CO), associated with smoke backlayering.

Disclaimer: The findings and conclusions in this report are those of the authors and do not necessarily represent the views of the National Institute for Occupational Safety and Health.

Abstract

To determine the critical air velocity for preventing smoke rollback, diesel-fuel fire experiments were conducted in the National Institute for Occupational Safety and Health's (NIOSH) Pittsburgh Research Laboratory's Safety Research Coal Mine. Such information is necessary for preplanning and implementation of ventilation changes during mine fire fighting and rescue operations. The fire intensity varied from 50 to 300 kW depending on the fuel tray area. Airflow in the 2-m- (6.6-ft-) high, 2.9-m- (9.5-ft-) wide coal mine entry was regulated during the course of each experiment. The airflow was measured upwind from the fire as an average over the entry cross-section with an ultrasonic airflow sensor and was recorded dynamically with a mine monitoring system. The extent of smoke reversal was monitored with light-obscuration monitors, ionization smoke sensors and visual observations. Experimental results for the critical air velocity for smoke reversal as a function of fire intensity compared very well with model predictions based upon a computational fluid dynamics fire dynamics simulator.

FIGURE 1

Plan view of mine test section.

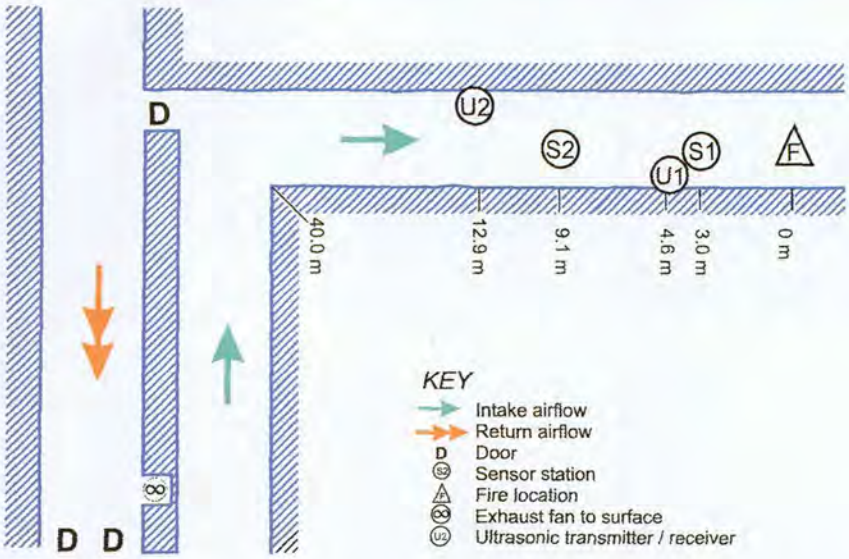

In the absence of remote real-time ventilation and POC monitoring, the selection of a ventilation change is not without unknown risks. To meet the objective of establishing a safe procedure for ventilation induced smoke control, an experimental and a computational modeling approach was undertaken to determine the critical ventilation velocity required to prevent smoke reversal from fires of specific heat intensities. This information will be useful for preplanning and implementation of ventilation changes under emergency conditions. Experimental studies on smoke backlayering from a tunnel fire and determination of the critical velocity to prevent smoke backlayering were conducted in a large tunnel (Massachusetts Highway Department, 1995), with a hydraulic diameter of 7.75 m (25.4 ft), and in small tunnels, with hydraulic diameters between 0.18 and 0.40 m (0.6 and 1.3 ft) (Wu and Baker, 2000).

Experiments in mine-size tunnels with hydraulic diameters of 2.38 m (7.8 ft) were conducted at Buxton (Wu and Baker, 2000) with fire intensities greater than 200 kW. None of these cases were conducted in a mine entry, which because of their rough walls introduces additional turbulence. This research considers fire intensities of less than 300 kW in a coal mine entry for an evaluation of the critical velocity to prevent smoke reversal. The practical experimental limitations of experiments for large fire intensities necessitates the use of a predictive computational method to extrapolate limited experimental results to a range of fire intensities and mine entry dimensions not practically achievable experimentally.

Modeling approaches can be semi-empirical analytic models or field models that depend on a numerical evaluation of the Navier-Stokes equations with a computational fluid dynamics (CFD) program. Kennedy et al. (1996) developed a one-dimensional analytic model to investigate the critical ventilation velocity required to prevent smoke reversal. The model depends on an estimate of the Froude number to prevent smoke reversal. Mitchell (1996, page A-2) proposed a simple relationship for estimating the critical velocity for smoke rollback in relation to the entry height, but independent of fire intensity. Wu and Bakar (2000) used a field model to determine the dependence of the critical velocity on fire intensity for laboratory-scale tunnel fires. A CFD approach will also predict the length of the smoke backlayer for subcritical air velocities. The length of stationary smoke backlayer as a function of fire intensity and ventilation velocity has been modeled by Hwang and Edwards (2001) with a CFD computer program.

Experimental procedure

The entry selected for the smoke-reversal experiments was 126 m (413 ft) long, had an average height of 2.06 m (6.76 ft) and a width of 2.91 m (9.55 ft). The entry was formed from a right-angle bend with the intake portal. Figure 1 shows a plan view of the fire location and the doors used for regulating the airflow. The fire was located 40 m (130 ft) downwind from the bend. The ratio of this 40-m (130-ft) distance to the airway hydraulic diameter was 17, which assured that the turbulent flow velocity was uniform. Five-point vane anemometer measurements made over the entry cross section at the fire zone indicated this to be the case. The slope of the airway upwind and downwind from the fire was less than 0.2° and was, therefore, inconsequential for smoke movement along the roof.

The fire source on the entry floor consisted of a pan containing diesel fuel. To control the heat-release rate, the fire pan surface areas ranged from 0.09 to 0.49 m^2 (1 to 5.3 sq ft) for the experiments. Monitoring of the smoke reversal was accomplished with two sensor stations located 3 and 9.1 m (10 and 30 ft) upwind from the fire source, as well as markers spaced every 1.52 m (5 ft) upwind from the fire along the rib for visual observation. At each sensor station, a light obscuration monitor was suspended approximately 0.5 m (1.5 ft) from the roof, above which was positioned an ionization smoke sensor. Approximately 4.6 m (15 ft) upwind from the fire source, near the roof and rib, was a transmitter-receiver of the ultrasonic airflow measurement sensor. The other transmitter-receiver was located 8.28 m (27 ft) upwind on the entry's opposite rib near the floor. The acoustic airflow and smoke indication sensor outputs were sampled every two seconds by the mine monitoring system.

Measurements

The fire effective tray sizes are listed in Table 1 for each experiment. For each experiment, the tray was centered on the entry floor relative to the ribs with the longer side positioned transverse to the entry. In Experiments C, E and F, two trays were positioned adjacent to each other to form the effective tray area. The fire intensities and fuel mass fluxes were calculated from visual observation of the duration of flaming combustion for known fuel quantities and the physical and chemical properties of the diesel fuel. The diesel fuel's mass density was 876

kg/m^3, and the heat of combustion was 42.31 MJ/kg. Ignition was achieved by first pouring a small quantity (about 200 mL) of heptane on the diesel fuel. Prior to ignition, the airflow was measured with a vane anemometer at the fire tray. A five-point measurement was made at the airway center and corners. An average of these results was compared with the average acoustic measurement of the air velocity over the same time interval. For Experiments A, B and D the relative error was less than 1.2 percent, for Experiment C the relative error was 4.5 percent, for Experiment E the relative error was 7.2 percent and for Experiment F the relative error was 3.6 percent.

Table 1

Fire pan size and interpolated fire intensity.

Experiment size, m	Effective tray L	Fuel, Q, kW	Fire intensity	Mass flux kg/s/m^2
A	0.46 X 0.46	9.1	130	0.0147
B	0.61 X 0.61	15.1	267	0.017
C	1.07 X 0.46	20.8	304	0.0142
D	0.39 X 0.23	3.8	53	0.0155
E	0.79 X 0.23	7.6	102	0.0148
F	0.46 X 0.39	7.6	128	0.0187

Figure 2 shows the responses of the light monitor (LIGHT) and smoke sensor (SMOKE) 3 m (10 ft) upwind from the 130-kW fire for Experiment A and shows the response of the ultrasonic flow measurement instrument. The LIGHT and SMOKE values are normalized by their prefire ambient values. Also shown are several visually observed positions of the smoke roll back marked by the curve labeled EVENT. The extent of the smoke roll-back is noted above the EVENT curve in Figs. 2 and 3.

The light monitor as an optical device has a faster response to the presence of smoke particulates and their clearing than the diffusion mode smoke sensor. From 9:04 to 9:08 a.m., the smoke was in the neighborhood of the sensors 3 m (10 ft) upwind from the fire pan. Instability in the roll back of the buoyancy-generated smoke resulted in significant fluctuations in the light and smoke sensor responses. Over this time period, the ratio of the average signal to the signal's standard deviation was about 44 for the flow sensor, with reduced ratios of 11 for the light monitor and 3 for the smoke sensor. This illustrates how, for even a relatively steady airflow, the fire's fluctuating thermal effects will be amplified in the smoke movement.

The ventilation velocity at the flow measurement device was 0.54 m/sec (1.8 ft/sec) when the smoke backlayer extended 6.1 to 9.1 m (20 to 30 ft), 0.86 m/sec (2.8 ft/sec) when the backlayer extended 3 m and 1.19 m/sec (3.9 ft/sec) when the smoke was maintained at the fire pan. These velocities are converted to average velocities at the fire pan based on the 5.27 m^2 (56.7 sq ft) entry cross-sectional area at the fire pan and 6.09 m^2 (65.6 sq ft) cross-sectional area at the flow monitor. The critical airflow at the fire pan for no smoke reversal is, accordingly, 1.38 m/sec (4.5 ft/sec). The restriction to human visibility posed by the smoke backlayer can be estimated from the output of the light obscuration monitor. At the reduced airflow of 0.63 m/sec (2.1 ft/sec) at the fire pan from 9:00 to 9:01:50 a.m., which is a 54 percent reduction in the ventilation velocity from its critical value, the average optical density of the smoke was 0.95 and 0.31 m^{-1} at the light monitors 3.0 and 9.1 m (10 and 30 ft) upwind from the fire. These optical densities correspond to visibilities of 3.7 and 11.3 m (12.1 and 37.1 ft), respectively, based on Jin's (1977) relationship between visibility measured relative to a light-emitting sign and the optical density. For a light-reflecting sign, the associated visibilities are 1.4 and 4.2 m (4.6 and 13.8 ft).

Jin (1977) also notes that a minimum visibility of 3 to 5 m (10 and 16 ft) is required for fire-escaping personnel familiar with the surroundings, and a visibility of 15 to 20 m (50 to 66 ft) is required for personnel unfamiliar with the surroundings. Reliance on a cap lamp's reflection from mine entry markings would be characteristic of reflection from a light reflecting sign. This shows the visibility limitation due to a relatively small 130-kW fire for someone familiar with the mine who, for mine escape, needs to rely on a light from a cap lamp reflecting from mine entry markings.

Figure 3 shows similar results for the 304-kW fire of Experiment C. The constant values for the measured airflow from 9:10 to 9:14 a.m. and from 9:28 to 9:34 a.m. are

FIGURE 2

Optical and smoke sensor dimensionless response at the 3-m (10-ft) station and airflow measurement for Experiment A.

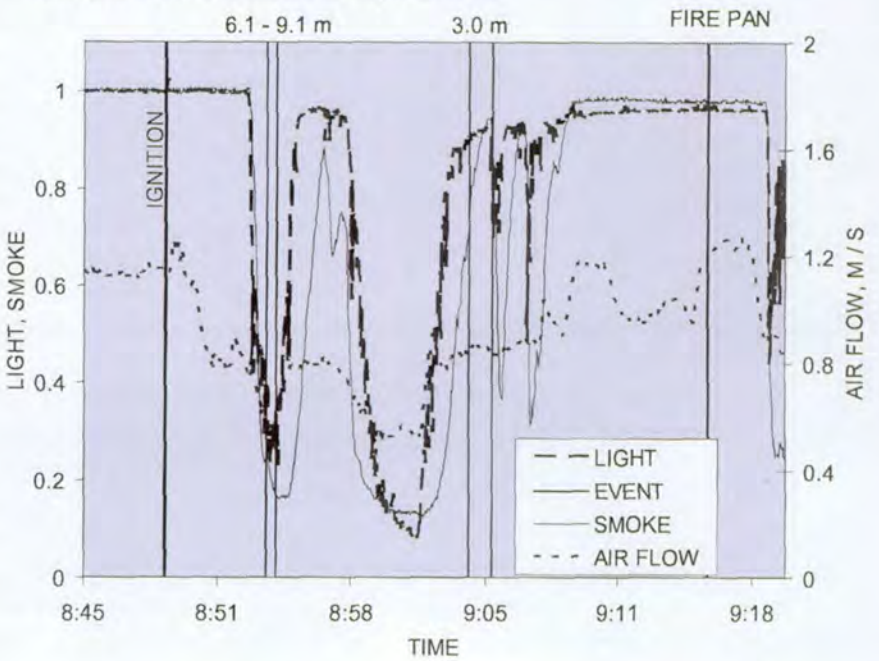

FIGURE 3

Optical and smoke sensor response at the 3-m (10-ft) station and airflow measurement for Experiment C.

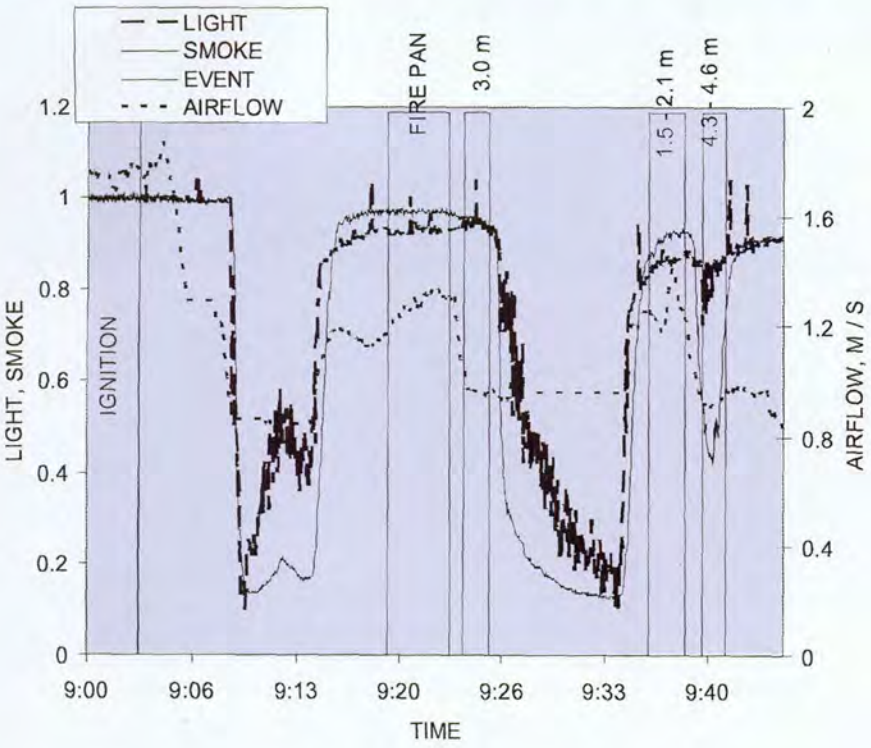

the result of very dense smoke, which causes attenuation and refraction of the ultrasonic acoustic transmissions between the transmitter and receiver. For Experiment C, the ventilation velocity at the ultrasonic flow measurement device was 1.28 m/sec (4.2 ft/sec) when the smoke was stabilized at the fire pan. This corresponds to a 1.55 m/sec (5.09 ft/sec) flow velocity at the fire pan. A stationary roof smoke backlayer of 3 m (10 ft) developed for a ventilation of 0.97 m/sec (3.18 ft/sec), as indicated by the flow measurement sensor, and a 4.3 to 4.6 m (14 to 15 ft) backlayer developed for a ventilation of 0.93 m/sec (3.1 ft/sec). Table 2 lists the critical velocity, V_c, at the fire pan to prevent smoke rollback for the six experiments. For the six experiments with a fire intensity range from 53 to 304 kW, the ratio of the critical velocity to the velocity representative of a 3 m (10 ft) backlayer was 1.25, with a standard deviation of 0.1.

It is instructive to represent the relationship between critical air velocity Vc and fire intensity Q, as dimensionless quantities, for both calculated and experimental values of V_C and Q. The dimensionless critical air velocity V_C^* and heat release rate Q^* are defined by (Wu and Baker, 2000)

$$V_c^* = \frac{V_c}{\sqrt{gH}} \qquad (1)$$

$$Q^* = \frac{Q}{\rho_0 T_0 C_p \sqrt{gH^5}} \qquad (2)$$

where

ρ_0 is the inlet ambient air density,

T_0 is the inlet ambient temperature,

C_p is the air specific heat (1.005 kJ/kg/K) and

g is the acceleration due to gravity (9.8 m/s^2).

The characteristic length H is the hydraulic diameter of the entry. It is defined as four times the ratio of the entry cross-sectional area to entry perimeter. For Experiments C through F, a thermal insulating material was attached to the roof at the fire location to protect the mine monitoring system data transmission cables from thermal damage. This reduction in the entry height at the fire pan accounts for variations shown for the hydraulic diameter, H, in Table 2. Although these dimensionless variables account for the entry height and width through the hydraulic diameter, they do not account for the fire shape.

Figure 4 shows the dependence of the dimensionless critical velocity on the dimensionless heat release rate. The literature (Thomas, 1970; Massachusetts Highway Department, 1995) shows a dependence of V_c on Q to the one-third power. The trend line in Fig. 4 shows a power dependence equal to 0.3, which is in reasonable agreement with the theoretical one-third value. The R-squared value, the square of the coefficient of correlation, was equal to 0.89. Shown for comparison are the dimensionless values reported for the experiments of Wu and Bakar (2000), and the values they report for experiments conducted at Buxton over the comparable Q^* range from zero to 0.04.

The dimensionless critical velocities for the SRCM experiments are higher than the Buxton and the Wu and Bakar values. Both the SRCM and Buxton experiments used a tunnel with comparable hydraulic diameters. For the Buxton gallery experiments, the hydraulic diameter was 2.38 m (7.8 ft). For the SRCM experiments, the hydraulic value was 2.15 m (7.05 ft) with thermal insulation at the roof and 2.27 m (7.45 ft) without thermal insulation at the roof. A significant difference between the experiments was the arch-shaped roof of the Buxton tunnel and the flat roof of the SRCM entry.

Table 2

Mine fire critical velocity, dimensionless critical velocity and fire intensity.

Experiment	Fire intensity, kW	V_c, m/s	H, m	Q^*	V_c^*
A	130	1.38	2.27	0.016	0.29
B	267	1.51	2.27	0.032	0.32
C	304	1.55	2.21	0.038	0.33
D	53	0.92	2.15	0.0070	0.20
E	102	1.08	2.15	0.0135	0.23
F	128	1.32	2.15	0.0171	0.29

Visual observations in the SRCM experiments indicated the visible flames did not fill the entry cross-section. The small tunnels used for the Wu and Bakar (2000) experiments had hydraulic diameters between 0.25 and 0.4 m (0.82 and 1.31 ft). Wall roughness is a significant factor in the SRCM entry, whereas the other tunnels were smooth walled. The fire intensities associated with the kerosene fires in the Buxton gallery were between 0.3 and 20 MW, while those for the propane source fires in the Wu and Bakar experiments were between 1.4 and 28 kW. Another factor that contributes to the difference in the experiments is the geometry of the fire source.

Associated with smoke reversal is the roof layer's elevated temperature, which is characteristic of the smoke's buoyancy. For Experiment E, the 102-kW fire, when the smoke had stabilized 12.2 m (40 ft) upwind from the fire, the smoke temperature at the roof was 66° C (150° F) above the fire and was 59° and 54° C (138° and 129° F), respectively, 1.52 and 3 m (5 and 9.8 ft) upwind from the fire. For Experiment F, the 128-kW fire, when the smoke had stabilized 7.62 m (25 ft) upwind from the fire, the smoke temperature near the roof was 80° C (176° F) above the fire and 61° and 58° C (142° and 136° F), respectively, 1.52 and 5 m (5 and 16.4 ft) upwind from the fire. At a location 10.2 m (33.5 ft) downwind from the fire, the air temperature near the roof was 41°C (106°F). The ambient temperatures were 22° and 20° C (72° and 68° F) for Experiments E and F, respectively. This corresponds to Thomas's (1970) observation that reverse flow is associated with hot smoke and not cold smoke. This condition can be quantified by the Froude number, Fr, which is defined as

$$Fr = \frac{gh\left(\frac{1-T}{T_f}\right)}{V^2} \qquad (3)$$

where
T_f is the hot gas layer temperature,
T is the ambient temperature in (K),
h is the tunnel height,
g is the gravitational acceleration and
V is the ventilation velocity.

Application of mass and energy conservation equations with the Froude numbers equal to 4.5 by Kennedy et al. (1996) leads to the predicted values shown in Fig. 4 for critical velocity. The selection of a Froude number equal to 4.5 was based on scale-model tests in ducts by Lee et al. (1979a; 1979b). The SRCM fire tests results are more realistically modeled with Fr = 0.75, as shown in Fig. 4.

Mitchell (1996, page A-2) presents a rule-of-thumb for the critical velocity to prevent smoke rollback. Expressed in feet per minute (fpm), the critical velocity is determined by

$$V_c = 100\sqrt{h} \qquad (4)$$

where
h is the entry height (ft).

When converted to dimensionless units with the identification of the hydraulic diameter with the entry height, the expression is $V^* = 0.29$. This value is independent of the heat release rate and is shown as a constant value curve in Fig. 4. For Q^* values less than 0.022, the Mitchell estimate provides adequate ventilation for the prevention of smoke rollback for the SRCM fires. For Q^* values greater than 0.022, the Mitchell result underestimates the required ventilation for the prevention of smoke rollback. A Q^* value equal to 0.022 corresponds to a 135-kW fire for an entry with a 2-m (6.6-ft) hydraulic diameter.

FIGURE 4

Dimensionless critical velocity dependence on dimensionless heat release rate.

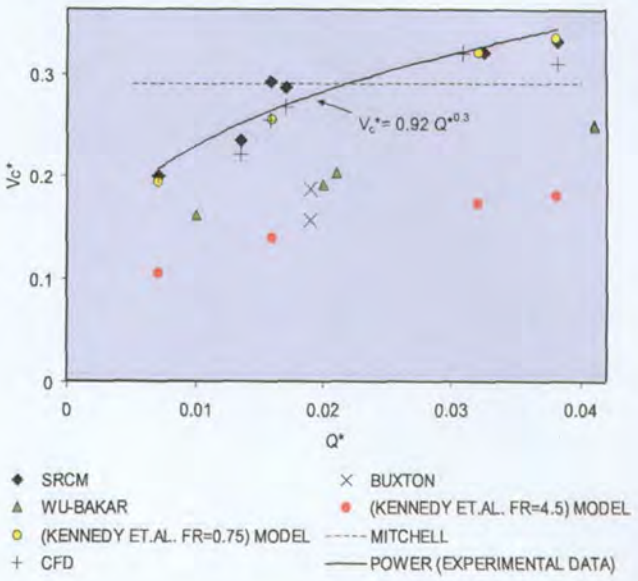

Modeling

The National Institute of Standards and Technology (NIST) (McGrattan et al., 2002) developed a CFD model of fire-driven fluid flow. NIST'S fire dynamics simulator (FDS) is a numerical simulator for low Mach number flows with special applications to heat and smoke transport. The program solves the Navier-Stokes equations numerically for fluid flow with a mixture fraction combustion model. A significant feature of the program is the large-scale eddy simulation (LES) method for turbulence. FDS was applied to a simulation of the six fire experiments conducted in the SRCM at PRL. The dimensions for the fuel tray and entry average cross section were entered in detail. A 50-m (164-ft) length of tunnel section was used in the simulation with the fire located 30 m (100 ft) downwind from the entrance. The critical velocity for the experiment is determined from the analysis of the airflow at the roof. When the airflow at the roof does not extend upwind from the leading edge of the fire source, the inlet flow is at the critical velocity. For these computations, a 20-second time average over the last 20 seconds of a five-minute time interval was used to define the stationary state. These values were determined to be close to two-minute time interval computations. Figure 4 shows good agreement between the SRCM experimentally determined critical velocity and the CFD predictions with FDS.

Although the instability of the smoke reversal made it

FIGURE 5

Dimensionless correlation of smoke reversal length with fire intensity.

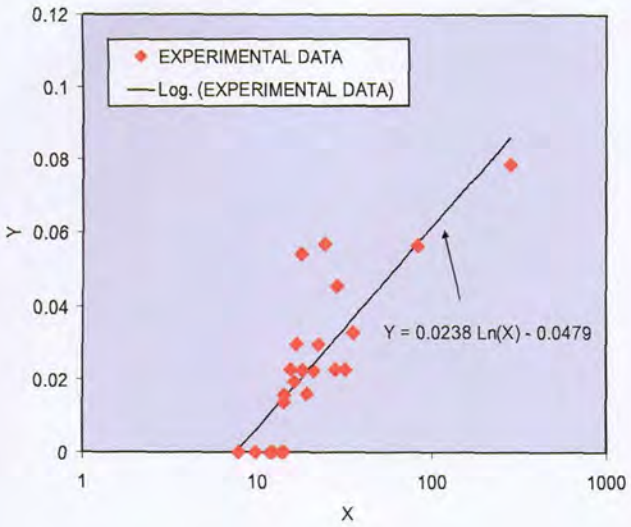

difficult to define with great certainty, the extent of smoke reversal for different ventilation velocities, a reduction of the data with dimensionless variables makes the trend more apparent. For the smoke reversal length L achieved for different ventilation velocities V_{in} and heat release rates Q, a pair of dimensionless variables, X and Y, can be defined as

$$X = \frac{Q}{AV_{in}^{3}\rho_0} \tag{5}$$

$$Y = \frac{L}{H}\frac{gH}{C_p\left(T_f - T_0\right)} \tag{6}$$

where
T_f is the flame temperature (K).

Figure 5 shows the parameters X and Y for the available experimental data. For this evaluation, the flame temperature was set to 1,600K. The correlation between X and Y satisfies the simple relationship $Y = 0.0238 \ln(X) - 0.0479$ with a R-Squared value, the square of the coefficient of correlation, equal to 0.68. The constant coefficients will change inversely with the selected flame temperature. The data for the six different fire intensities in the range 7.8 to 14.1 for $L = 0$ ($Y = 0$) is representative of the critical air velocity to prevent smoke reversal.

Conclusions

It was demonstrated with fire smoke reversal experiments in the NIOSH SRCM that for a range of fire intensities between 50 and 300 kW in a 2-m- (6.6-ft-) high, 2.9-m- (9.5-ft-) wide mine entry that the critical velocity for preventing the development of a smoke layer upwind from the fire is proportional to the fire intensity to the 0.3 power. This is in substantial agreement with other researchers who posit a one-third law dependence on the fire intensity.

The development of visibility obscuration 9 m (30 ft) upwind from a small 130-kW fire when the ventilation velocity was reduced by 54 percent from its critical value demonstrated the importance for maintaining the critical ventilation velocity for smoke control. For the fires considered, the results are in approximate agreement with an empirical result that is independent of fire intensity. CFD modeling of the dependence of the critical air velocity on fire intensity showed good qualitative agreement with measured values as shown in Fig. 4. ■

References

Code of Federal Regulations, 2002, "30CFR, Part 57.4761," Office of the Federal Register, National Archives and Standards Administration, U.S. Government Printing Office, Washington, D.C., July 1, 2002.

Hwang, C.C., and Edwards, J.C., 2001,"CFD modeling of smoke reversal," *Proceedings of the International Conference on Engineering Fire Protection Design, Society of Fire Protection Engineers*, Bethesda, MD, pp. 376-387.

Jin, T., 1977, "Visibility through fire smoke," *Journal of Fire & Flammability*, Vol. 9, pp. 135-155.

Kennedy, W.D., Gonzales, J.A., and Sanchez, J.G., 1996, "Derivation and application of the SES critical velocity equations," *ASHRAE Transactions: Research*, Vol. 102, No.2, pp. 40-44.

Lee, C.K., Chaiken, R.F., and Singer, J.M., 1979a, "Interaction between Duct fires and ventilation: an experimental study," *Combustion Science and Technology*, Vol. 20, pp. 59-72.

Lee, C.K., Hwang, C.C., Singer, J.M., and Chaiken, R.F., 1979b, "Influence of passageway fires on ventilation flows," Second International Mine Ventilation Congress, Reno, NV.

Massachusetts Highway Department, 1995, "Memorial Tunnel Fire Ventilation Test Program, Test Report," Boston, MA.

McGrattan, K.B., Forney, G.P., Prasad, K., Floyd, J.E., and Hostikka, S., 2002, "Fire Dynamics Simulator (Version3)-User's Guide," U.S. Dept. of Commerce, National Institute of Standards and Technology.

Mitchell, D.W, 1996, Mine Fires Prevention, Detection, Fighting, Intertec Publishing Inc, Chicago, IL, pp.19-20

Thomas, P.H., 1970, "Movement of smoke in horizontal corridors against an airflow," *Inst. Fire Engrs.* Q., Vol. 30, pp. 45-53.

Wu, Y., and. Bakar, M.Z.A., 2000, "Control of Smoke flow in tunnel fires using longitudinal ventilation systems—A study of the critical velocity," *Fire Safety Journal*, Vol. 35, pp. 363-390.

TRANSACTIONS

OF

SOCIETY FOR MINING, METALLURGY, AND EXPLORATION, INC.

Volume 320

2006

Editor

William R. Yernberg

PUBLISHED BY SME INC.

AT THE OFFICE OF THE EXECUTIVE DIRECTOR

8307 Shaffer Parkway

Littleton, Colorado 80127

Printed in the United States of America

ISBN-13: 978-0-87335-255-0 ◊ ISBN-10: 0-87335-255-6